# Broad absorption features in wind-dominated ULXs?

Matthew J. Middleton[1], Dominic J. Walton[2], Timothy P. Roberts[3] and Lucy Heil[1]

1. *Astronomical Institute Anton Pannekoek, Science Park 904,1098 XH, Amsterdam, Netherlands*
2. *Astronomy Department, California Institute of Technology, 1200 East California Boulevard, Pasadena, California 91125, USA*
3. *Department of Physics, University of Durham, Durham DH1 3LE, UK*

1 November 2013

**ABSTRACT**

The luminosities of ultraluminous X-ray sources (ULXs) require an exotic solution with either super-critical accretion modes onto stellar mass black holes or sub-critical accretion onto intermediate mass black holes (IMBHs) being invoked. Discriminating between the two is non-trivial due to the present lack of a direct mass measurement. A key expectation of the super-critical mode of accretion is the presence of powerful radiatively-driven winds. Here we analyse *XMM-Newton* data from NGC 5408 X-1 and NGC 6946 X-1 and find that strong soft residuals present in the X-ray spectra can be reconciled with broadened, blue-shifted absorption by a partially ionised, optically thin phase of this wind. We derive initial values for the physical parameters of the wind; we also discuss other possible origins for the observed features.

**Key words:** accretion, accretion discs – X-rays: binaries, black hole

## 1 INTRODUCTION

Recent studies of ultraluminous X-ray sources (ULXs: Roberts 2007; Feng & Soria 2011) in nearby galaxies have shown that up to $\sim3\times10^{39}$erg s$^{-1}$, their luminosities can be robustly associated with accretion around the Eddington limit onto stellar mass ($<$ 100 M$_\odot$) black holes (e.g. Middleton et al. 2012, 2013). Those with luminosities reaching $\sim3\times10^{40}$ erg s$^{-1}$ are harder to explain yet seem to show a trend of spectral shape with variability (Sutton, Roberts & Middleton 2013). Their behaviour appears strikingly dissimilar the expected behaviour of sub-Eddington Galactic black hole binaries scaled up into the intermediate-mass black hole regime (IMBHs; Colbert & Mushotzky 1999, with masses $>$100 M$_\odot$), implying they cannot *all* be IMBHs unless the characteristic properties of accretion alter dramatically beyond the expectations of simple mass scaling.

The behaviour of most bright ($3$-$30\times10^{39}$ erg s$^{-1}$) ULXs can plausibly be explained by stellar mass black holes undergoing accretion in the 'super-critical' regime (Shakura & Sunyaev 1973). In this situation, the inflow changes at the radius where the accretion rate is locally Eddington. This drives an increase in scale height of the disc and optically thick winds to be radiatively launched from the surface (Poutanen et al. 2007; Dotan & Shaviv 2011; Ohsuga & Mineshige 2011) which are likely to be stratified due to the Rayleigh-Taylor or radiative-hydrodynamic instabilities (Takeuchi et al. 2013). The presence of such winds are predicted to affect the spectrum (Poutanen et al. 2007), observed luminosity (King 2009) and variability (Middleton

et al. 2011) depending on inclination angle to the observer's line-of-sight and changing mass accretion rate (which we will describe fully in a forthcoming model).

Observations show that narrow atomic features in emission or absorption (namely Fe K$_\alpha$) must be intrinsically weak or simply not present in two of the hardest (and brightest) ULXs (Walton et al. 2012; 2013). However, in the super-critical wind model, these 'hard ultraluminous' ULXs are those that we view close to face-on (Sutton et al. 2013). The 'soft ultra luminous' ULXs that display far higher levels of fractional variability, are thought to be viewed such that the line-of-sight to the hottest inner regions are obscured by the optically thick phase of the clumpy wind (i.e. scattered out of the line-of-sight: Middleton et al. 2011; Middleton et al. in prep). It is therefore these 'soft ultraluminous' sources where we should expect to see atomic absorption features, the expected signatures of such outflows.

Interestingly, it has long been known that soft spectrum ULXs can show strong residuals to their best fitting continuum models (e.g. Stobbart, Roberts & Wilms 2006 and references therein), which have traditionally been associated with emission from collisionally heated gas in the host Galaxy. However, the intrinsic luminosities in such components are very large (approaching $\sim1\times10^{39}$ erg s$^{-1}$) and such residuals are seen in ULXs without large amounts of host galactic diffuse emission (Bachetti et al. 2013) leading some to question this identification (Middleton et al. 2011).

Here we investigate whether absorption in the wind can account for the spectral residuals in this subset of ULXs by studying two of the brightest members of the population.

**Table 1.** ULX observational information

| ULX | OBSID | obs. date | good time (ks) |
|---|---|---|---|
| NGC 5408 X-1 | 0302900101 | 2006-01-13 | 85.4 |
| | 0500750101 | 2008-01-13 | 28.6 |
| | 0653380201 | 2010-07-17 | 71.8 |
| | 0653380301 | 2010-07-19 | 88.2 |
| | 0653380401 | 2011-01-26 | 73.4 |
| | 0653380501 | 2011-01-28 | 69.2 |
| NGC 6946 X-1 | 0691570101 | 2012-10-21 | 81.1 |

Notes: *XMM-Newton* observation identifier, date of exposure, PN spectral exposure (after accounting for background flares and deadtime) for each observation studied.

## 2   WIND-DOMINATED ULXS

The most variable ULXs detected are NGC 5408 X-1 (Middleton et al. 2011; Heil, Vaughan & Roberts 2009; Pasham & Strohmayer 2012) and NGC 6946 X-1 (Rao et al. 2010), both with energy integrated fractional excess variances over intra-observation timescales of >20% (and up to ∼60%). Both sources are also known to harbour quasi-periodic oscillations (QPOs); although determining the mass based on association to those QPOs seen in BHBs (e.g. Strohmayer & Mushotzky 2009) has proven non-trivial (Middleton et al. 2011; Pasham & Strohmayer 2012).

The evolution of NGC 5408 X-1 over 6 deep *XMM-Newton* observations (spanning several years) has been well studied by Pasham & Strohmayer (2012) who found very little change in the X-ray spectra (although significant changes were found in the variability power spectra). The X-ray spectra show a strong soft thermal component, peaking below 1 keV with a tail of emission rolling over at 3-4 keV (such a break appears almost ubiquitously in high quality *XMM-Newton* ULX data: Gladstone et al. 2009 now confirmed by NuSTAR: Bachetti et al. 2013). In the super-critical framework the soft emission is from the wind (and photosphere), with the hard emission originating in a heavily distorted inner accretion disc (Poutanen et al. 2007). In addition to models describing the continuum, past studies have highlighted the need for an extra component to account for spectral residuals below 2 keV (e.g. Strohmayer & Mushotzky 2009). Should these be associated with a collisionally excited plasma (emitting as a Brehmstrahlung spectrum with overlaid emission lines) then the integrated luminosity is found to approach $\sim 1 \times 10^{39}$ erg s$^{-1}$. This is considerably brighter than predicted for the star-formation-related diffuse emission of the *entire* galaxy, inferred to be $\sim 3 \times 10^{37}$ erg s$^{-1}$ (see Dale et al. 2005; Calzetti et al. 2007; Mineo et al. 2012).

Middleton et al. (2011) proposed that the large amplitudes of rms and trend of fractional variability with energy seen in NGC 5408 X-1 could both be explained by optically thick, clumpy material in the wind obscuring sight lines to the inner disc (e.g. Takeuchi et al. 2013). In this scenario both the spectra and variability can be explained by super-critical accretion and are heavily influenced by the wind. NGC 6946 X-1 is not as well-studied as NGC 5408 X-1, however, Rao et al. (2010) have shown it to have both a similar X-ray spectrum and similar (in fact larger) amplitudes of rms variability on the same timescales. Given the close as-

sociation of variability and spectral behaviour in accreting sources (e.g. Muñoz-Daria et al. 2011) it is quite reasonable to assume both sources could be 'wind-dominated' ULXs.

## 3   SPECTRAL MODELLING

We re-processed the 6 *XMM-Newton* (EPIC MOS and PN) archival datasets of NGC 5408 X-1 (acquired from HEASARC (http://heasarc.gsfc.nasa.gov/)) and the latest (proprietary) observation of NGC 6946 X-1 using SAS 12 and up-to-date current calibration files (see Table 1 for details). We followed standard extraction procedures and filtered for soft proton flaring in the full-field, high energy (10-15 keV) background, extracting good time intervals (GTI). As the PN has the highest response to these events we used the PN GTI as input in extracting spectra, using XSELECT, confirming that this removes all flares in the equivalent MOS lightcurves. We selected ≥30 arcsec radius source and background regions with the latter selected to be on the same chip, free from sources and away from the readout direction of bright sources. The OBSIDs, observation dates and useful exposures are given in Table 1. Given that the spectra of NGC 5408 X-1 do not change by a large amount at soft energies where the residuals are seen, we combined the MOS (1 & 2 separately) and PN datasets using ADDASCASPEC. However, as the spectrum of NGC 6946 X-1 changes markedly compared to earlier, shorter observations, we focus our analysis only on the latest, deep observation.

We proceeded to initially model the continuum for each source in order to identify and study the residuals. To this end we used a suitable convolved model in XSPEC (Arnaud 1996) representative of emission from the outer wind (DISKBB) and emission from the inner hot disc (NTHCOMP: Zycki, Done & Smith 1999). The Compton component gives us the additional freedom to account for any putative Compton down-scattering in the wind (Titarchuk & Shrader 2005) which may act to distort the hot disc profile, extending it to lower energies (Middleton et al. in prep). We set the input seed photon temperature to be that of the lower temperature wind to ensure correct energy balance in the event of scattering and prevent further rollover at energies out of the bandpass (consistent with this model of accretion: Poutanen et al. 2007, and recently confirmed in *NuSTAR* observations by Bachetti et al. 2013). We included absorption by neutral ISM material (TBABS) with appropriate abundances (Wilms et al. 2000) and lower limit set to the Galactic line-of-sight column (NGC 5408: $6.0 \times 10^{20}$ cm$^{-2}$ and NGC 6946: $2.1 \times 10^{21}$ cm$^{-2}$; Dickey & Lockman 1990). As is standard practice we also included a constant component to account for differences between detector responses (usually <10% from unity except in the case of NGC 6946 X-1 MOS1 where a dead column across the source affected the spectrum).

The results of the spectral fitting are given in Table 2 and plotted in Figure 1. We confirm the presence of strong residuals in both NGC 5408 X-1 and NGC 6946 X-1 MOS and PN spectra. Following previous analyses of such residuals (e.g. Stobbart et al. 2006) we can model these as emission by a thermal plasma (APEC: Smith et al. 2001). Such models are sensitive to the heavy metal abundance, however this is uncertain in these sources; whilst observations of the NGC 5408 X-1 environment (Mendes de Oliveria et al. 2006)

**Table 2.** XSPEC model best-fit parameters

| ULX | $N_{\rm H}$ | $kT_{\rm d}$ | $\Gamma$ | $kT_{\rm e}$ | $\chi^2$ |
|---|---|---|---|---|---|
| | | | TBABS*(DISKBB+NTHCOMP) | | |
| 5408 X-1 | $0.092\pm0.003$ | $0.193 \pm 0.003$ | $1.65^{+0.12}_{-0.10}$ | $2.25 \pm 0.04$ | 2522/1663 |
| 6946 X-1 | $0.304^{+0.021}_{-0.020}$ | $0.232^{+0.015}_{-0.014}$ | $1.96 \pm 0.11$ | $1.63^{+0.31}_{-0.20}$ | 944/835 |

| ULX | $N_{\rm H}$ | $kT_{\rm apec}$ | $kT_{\rm d}$ | $\Gamma$ | $kT_{\rm e}$ | $\chi^2$ |
|---|---|---|---|---|---|---|
| | | | TBABS*TBVARABS*(APEC+DISKBB+NTHCOMP) | | | |
| 5408 X-1 | $0.052^{+0.009}_{-0.008}$ | $1.01 \pm 0.03$ | $0.152 \pm0.008$ | $2.36 \pm 0.06$ | $2.09^{+0.48}_{-0.29}$ | 1860/1661 |
| 5408 X-1 | $0.049 \pm 0.004$ | $1.02 \pm 0.02$ | $0.156 \pm 0.004$ | $2.36 \pm 0.03$ | $2.03^{+0.21}_{-0.16}$ | 1894/1661 |
| 6946 X-1 | $0.028^{+0.023}_{-0.021}$ | $1.14^{+0.07}_{-0.11}$ | $0.237\pm0.024$ | $1.98^{+0.07}_{-0.12}$ | $1.76^{+0.41}_{-0.25}$ | 788/833 |
| 6946 X-1 | $0.039^{+0.028}_{-0.025}$ | $1.14^{+0.07}_{-0.09}$ | $0.225^{+0.027}_{-0.025}$ | $2.00^{+0.11}_{-0.12}$ | $1.81^{+0.45}_{-0.27}$ | 785/833 |

| ULX | $N_{\rm H}$ | wind $N_{\rm H}$ | $log\xi$ | $z$ | $kT_{\rm d}$ | $\Gamma$ | $kT_{\rm e}$ | $\chi^2$ |
|---|---|---|---|---|---|---|---|---|
| | | | | TBABS*TBVARABS*XSTAR*(DISKBB+NTHCOMP) | | | | |
| 5408 X-1 | $0.028 \pm 0.005$ | $19.8^{+23.9}_{-5.8}$ | $3.44^{+0.14}_{-0.10}$ | $-0.12 \pm 0.01$ | $0.208 \pm 0.007$ | $2.29 \pm 0.08$ | $1.76^{+0.36}_{-0.23}$ | 1997/1660 |
| 5408 X-1 | $0.028 \pm 0.003$ | $6.4^{+8.3}_{-1.5}$ | $3.18^{+0.05}_{-0.07}$ | $-0.12 \pm 0.01$ | $0.206 \pm 0.004$ | $2.29^{+0.04}_{-0.05}$ | $1.73^{+0.16}_{-0.13}$ | 1985/1660 |
| 6946 X-1 | $0.115^{+0.014}_{-0.022}$ | $100.0 (> 55.2)$ | $3.69^{+0.01}_{-0.11}$ | $-0.13^{+0.01}_{-0.02}$ | $0.237^{+0.019}_{-0.009}$ | $2.05^{+0.12}_{-0.14}$ | $1.95^{+0.57}_{-0.40}$ | 863/832 |
| 6946 X-1 | $0.132^{+0.034}_{-0.021}$ | $41.9^{+4.2}_{-1.11}$ | $3.52^{+0.17}_{-0.06}$ | $-0.13 \pm 0.01$ | $0.218^{+0.015}_{-0.021}$ | $2.12^{+0.16}_{-0.12}$ | $2.14^{+2.73}_{-0.46}$ | 838/832 |

Notes: Units of $N_{\rm H}$ are $10^{22}$ cm$^{-2}$ and temperatures (seed photons: $kT_{\rm d}$ and electron plasma: $kT_{\rm e}$) are quoted in keV. *Top:* Best-fit model parameters (and 90% errors) for the continuum model. *Middle:* model parameters when including thermal plasma emission with variable abundances (0.5 Z$_\odot$ top and Z$_\odot$ bottom).*Bottom:* when including absorption in a wind with a velocity dispersion of 0.1c, outflow velocity of $z\times$c and 0.5 Z$_\odot$ and Z$_\odot$ (top and bottom sets of values in each case).

implies sub-solar abundance, X-ray spectral fitting (Winter et al. 2007) measures abundances closer to solar (there are no equivalent constraints for NGC 6946 X-1 although the galactic metallicity is $\sim$ solar: Moustakas et al 2010). To account for these uncertainties we tested abundances set at 0.5 Z$_\odot$ and Z$_\odot$. In order to be fully consistent we included a second, variable abundance absorption column (TBVARABS) where we fixed the heavy metals (above He) to the abundance in the APEC component, redshift to zero and the column density of the TBABS component to its Galactic value. The model fitting (Table 2) gives thermal plasma luminosities of 3.9-5.3 (NGC 5408 X-1) and 2.8-5.6$\times10^{38}$ erg s$^{-1}$ (NGC 6946 X-1) for Z$_\odot$ and 0.5 Z$_\odot$; far greater than the inferred diffuse luminosity of either galaxy (Dale et al. 2005; Mineo et al. 2012) given the ratio of extraction region area to the projected galaxy area: $\sim1\times10^{37}$erg s$^{-1}$.

Should the residuals instead be the result of absorption in the line-of-sight by an outflowing, optically thin phase of a super-critical wind then by making some basic assumptions we can model these features using a table made with XSTAR2XSPEC (Kallman & Bautista 2001). Based on the simulations of Takeuchi et al. (2013) we may expect wind element sizes of $\sim$10 R$_{\rm s}$. If we (naively) assume that the column density of winds in BHBs when extremely bright ($\sim10^{24}$ cm$^{-2}$, e.g. Revnivtsev et al. 2002) is of order what we may expect to see in ULXs then this places an upper limit on the particle density of $10^{17}$cm$^{-3}$. As this upper limit gives a Thompson scattering optical depth $\leq$1 at these columns, we are satisfied that this is an appropriate, albeit crude value to use in this initial modelling. We used the best-fitting de-absorbed model to the continuum to provide the input, ionising flux, and produced four grids per source, stepping between log$\xi$ of 3 to 4 in five linear steps and column density of $1\times10^{22}$ -

$1\times10^{24}$ (limited so that the optical depth is less than unity) in eight logarithmic steps. As we do not know the velocity dispersion *a priori* we set the turbulent velocity (as a proxy for velocity dispersion) in the wind to be 0.01c and 0.1c (the predicted outflow velocity is an obvious upper limit: Takeuchi et al. 2013) and produced grids at 0.5 Z$_\odot$ and Z$_\odot$. In all grids we set the covering fraction to be unity as a limiting case. Fitting the resulting grids with the continuum (again using TBVARABS with matching abundances) in XSPEC we find the larger velocity dispersion of 0.1c to be statistically favoured (by $\Delta\chi^2 > 50$). Whilst including smeared absorption yields a highly significant improvement in $\Delta\chi^2$ from the continuum model (Table 2), this is evidently not as great as that obtained by including a thermal plasma (in both cases the fit quality remains poor for NGC 5408 X-1). However, we attribute this (and the spectral residuals in Figure 1) to the simplicity of our model; it only accounts for a single phase of the absorber (we do not fit multiple grids to avoid compounding caveats) yet there are likely to be multiple phases of differing densities (Takeuchi et al. 2013).

At the relatively high ionisation states inferred for the wind, H and He have no effective opacity and do not affect the shape of the spectrum. As a result, the different abundances in the grids are somewhat balanced by column density and ionisation state. Although we cannot be certain of the correct abundance at this time, we can use both best-fitting models (the parameters of which are given in Table 2) to determine the likely range of parameters for the wind. Given the particle density and range of log$\xi$ we can obtain a rough estimate for the location of the material relative to the central illuminating source. This explicitly assumes that the wind is exposed to the same de-absorbed, 0.3-10 keV X-ray luminosities that we observe: 7.7 and 7.6 $\times10^{39}$ erg s$^{-1}$
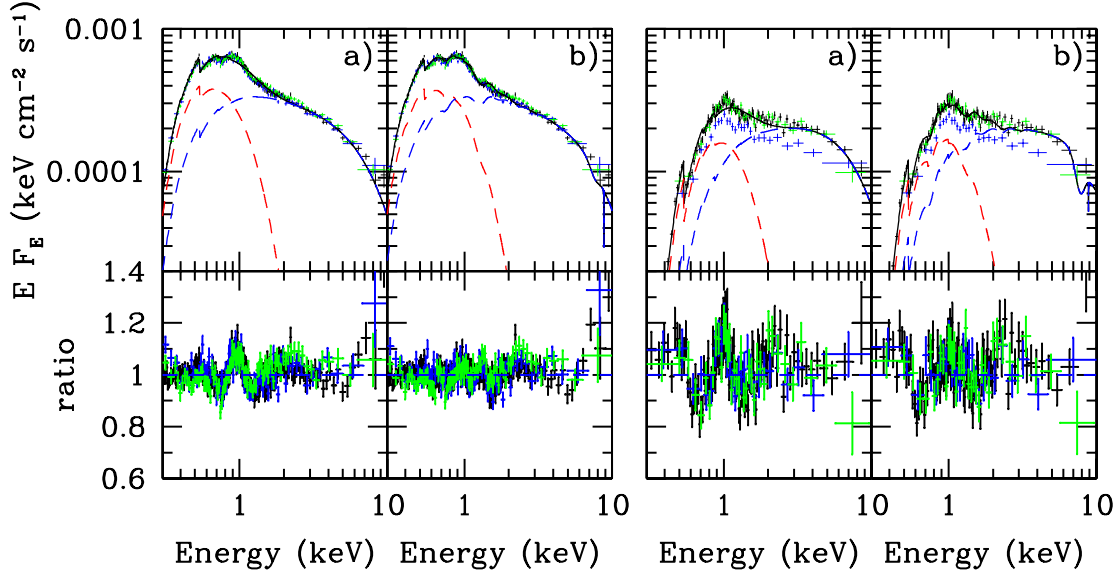
**Figure 1.** *Left a):* Best-fitting continuum model (DISKBB: red dashed line, NTHCOMP: blue dashed line) to the combined data for NGC 5408 X-1 (PN: black, MOS1: blue, MOS2: green) with model parameters given in Table 2. Residuals to the fit are shown in the panel below and clearly show an excess at 1 keV. *b):* Best-fitting model incorporating a partially ionised, optically thin wind (see Table 2 for best-fitting parameters), in this case with 0.5 $Z_\odot$. The residuals have been substantially reduced. *Right:* as for *left* with the data of NGC 6946 X-1 and best-fitting models. Note that the MOS1 data is lower due to the source region being affected by a dead column.

for NGC 5408 X-1 and NGC 6946 X-1 respectively (determined by integrating below the continuum model in Table 2). Following Tarter et al. (1969): $R \geq \sqrt{L_x/(\xi n_e)}$, we find $R > 5200$ $R_g$ and $> 3400$ $R_g$ for a 10 $M_\odot$ BH and for each source respectively (with the aforementioned caveats).

Using eqn 1 of Ponti et al. (2012) we can obtain a crude estimate for the mass outflow rate in this phase of the wind:

$$\dot{M}_w = 4\pi m_p v_{out} \frac{L_x}{\xi} \frac{\Omega}{4\pi} \qquad (1)$$

where $\Omega$ is the covering fraction of the wind, $m_p$ is the proton mass and $v_{out}$ is the outflow velocity. We can also estimate the mass inflow rate through the inner radius using the relations of Poutanen et al. (2007):

$$\dot{M}_o = M_{BH}^{-1/2} \left( \frac{1.5 f_c}{T_{c,sph} [\text{keV}]} \right)^2 \qquad (2)$$

$$\dot{M}_{in} \approx \frac{\dot{M}_o (1-a)}{1 - a \left( \frac{2}{5} \dot{M}_o \right)^{-1/2}} \qquad (3)$$

where $\dot{M}_o$ is the local mass accretion rate (in units of Eddington), $T_{c,sph}$ is the temperature at the wind spherization radius, $R_{sph}$, $f_c$ (the colour temperature correction due to Compton scattering) is assumed to be 1.7 (Poutanen et al. 2007), $a = \epsilon_w(0.83 - 0.25\epsilon_w)$ and $\epsilon_w$ is the fraction of radiative energy used to launch the wind. From the spectral fits we obtain $T_{c,sph}$ ($kT_d$). If we then assume the unphysical but limiting value of $\epsilon_w = 1$ (assuming maximal energy launches the wind and thus largest mass loss) and use the results of the model fitting, we obtain an upper limit on the mass outflow to inflow (to the BH) ratio of $< 1.1$ and $< 0.7$ for NGC 5408 X-1 and NGC 6946 X-1 respectively. In deriving the ratio we have assumed an accretion efficiency of 0.08 (standard for a Schwarzschild BH) with the values differing mostly due to the lower limit on log$\xi$ for NGC 5408 X-1. There are naturally several caveats e.g. this only accounts for this partially ionised phase of the wind, and the covering

fraction was set at unity (yet Walton et al. 2013 rule this out). We will explore these caveats in detail in a future work.

## 4  DISCUSSION & CONCLUSIONS

Given the bright nature of ULXs, it is natural to assign their properties to an exotic accretion scenario, either the presence of IMBHs or super-critical accretion modes onto stellar mass BHs. Assuming a common scaling of BH accretion physics (spectrum, variability, outflows etc.), the predictions for IMBHs are clear. At the inferred Eddington ratios we would expect generally hard spectra (rolling over well out of the *XMM-Newton* bandpass), with large amounts of fractional variability (e.g. Munoz-Darias et al. 2011). Whilst the amount of 'fast' variability in some ULXs seems to be an adequate match (though we caution that the QPOs do not yet provide a strong lever arm for identification), e.g. Caballero-Garcia et al. 2013, the spectra and behaviour seem to depart from expectation (see Gladstone et al. 2009; Sutton et al. 2013; Bachetti et al. 2013; Middleton et al. in prep). One thing is clear: at these accretion rates we do not expect IMBHs to be powering substantial winds (assuming scaling of accretion properties holds at these intermediate mass ranges). Conversely if we infer the presence of accretion onto stellar mass BHs we **must** invoke super-critical accretion and winds if we are to explain the bright ($3 < L_X < 30 \times 10^{39}$ erg s$^{-1}$) ULXs and their coupled spectra and variability (Sutton et al. 2013).

We can explain the large amounts of variability seen in some soft ULXs should they be 'wind-dominated', i.e. viewed at moderate inclinations, into the launching cone of the wind expected to accompany super-critical accretion (Middleton et al. 2011). In the cases of the two best observed of these, NGC 5408 X-1 and NGC 6946 X-1, strong residuals are seen at soft energies. Although these can be described by

thermal plasma emission, the luminosities appear improbably large for host galactic diffuse emission at the position of the source. If we instead associate these with collisionally excited circum-equatorial material (perhaps from earlier wind epochs) then we could generate the observed luminosities (Roberts et al. 2004). However, such emission should be isotropic, yet we appear to see these residuals predominantly in sources with soft spectra (and generally large amounts of fractional variability at high energies), e.g. the 'ULX dipper', NGC 55 ULX1 (Stobbart, Roberts & Warwick 2004). Conversely we note the overall lack of strong variability and residuals in those brightest and hardest ULXs thought to be viewed face-on (Sutton et al. 2013) which are also constrained to show only very weak (or no) narrow iron features (Walton et al. 2012; 2013). This could be a remarkable coincidence or else line-of-sight/inclination effects are an obvious solution (the lack of narrow emission in the hardest sources will be addressed in future work).

Our analysis has shown that absorption by an optically thin plasma, outflowing into the line-of-sight and ionised by the central source can broadly account for the residuals. We can reconcile this within the model of super-critical accretion where, at larger distances, the initially optically thick material in the wind disperses in the direction of the outflow (as the wind elements themselves are not in hydrostatic equilibrium) and becomes optically thin. Although the density of material drops, should the combination of distance from the ionising source and self-shielding (by the inner wind) allow the ionisation of the material to drop, we should see the effect of absorption by ionised species of abundant elements. Due to the velocity dispersion in the outflow, we would expect the lines to appear smeared and blue shifted when looking into the out-flowing path of the wind. In this way they are effectively analogous to the lines seen in BALQSOs at lower energies. Admittedly the model we have used is only simple (as can be seen from the moderately poor fit statistics) and lacks an accurate physical description of the outflow, radiative transfer and effect of self-shielding. However, this first step, whilst tentative, is still enlightening as it allows us to place initial constraints on certain physical parameters of the wind (which will be reviewed and updated as the models to describe the spectral imprint of these winds develop). Based on the results of our modeling we suggest that the optically thin wind is $>1000$ $R_g$ from the ionising source and may carry a large fraction of matter and energy from the accretion flow. We argue that this identification is the most likely and is the natural expectation of super-critical accretion. However, while this interpretation is the natural expectation for the super-critical regime, we are unlikely to be able to conclusively distinguish between this and other plausible explanations until the advent of missions carrying high throughput, high energy resolution instrumentation, e.g. Astro-H (Takahashi et al. 2010).

## 5   ACKNOWLEDGEMENTS

## REFERENCES

Arnaud K. A., 1996, ASPC, 101, 17
Bachetti M., et al., 2013, arXiv, arXiv:1310.0745
Caballero-García M. D., Belloni T. M., Wolter A., 2013, MNRAS, 2177
Calzetti D., et al., 2007, ApJ, 666, 870
Colbert E. J. M., Mushotzky R. F., 1999, ApJ, 519, 89
Dale D. A., et al., 2005, ApJ, 633, 857
Dickey J. M., Lockman F. J., 1990, ARA&A, 28, 215
Done C., Gierliński M., Kubota A., 2007, A&ARv, 15, 1
Dotan C., Shaviv N. J., 2011, MNRAS, 413, 1623
Feng H., Soria R., 2011, NewAR, 55, 166
Gladstone J. C., Roberts T. P., Done C., 2009, MNRAS, 397, 1836
Heil L. M., Vaughan S., Roberts T. P., 2009, MNRAS, 397, 1061
Kallman T., Bautista M., 2001, ApJS, 133, 221
King A. R., 2009, MNRAS, 393, L41
Mendes de Oliveira C. L., Temporin S., Cypriano E. S., Plana H., Amram P., Sodré L., Jr., Balkowski C., 2006, AJ, 132, 570
Middleton M. J., et al., 2013, Natur, 493, 187
Middleton M. J., Sutton A. D., Roberts T. P., Jackson F. E., Done C., 2012, MNRAS, 420, 2969
Middleton M. J., Roberts T. P., Done C., Jackson F. E., 2011, MNRAS, 411, 644
Mineo S., Gilfanov M., Sunyaev R., 2012, MNRAS, 426, 1870
Moustakas J., Kennicutt R. C., Jr., Tremonti C. A., Dale D. A., Smith J.-D. T., Calzetti D., 2010, ApJS, 190, 233
Muñoz-Darias T., Motta S., Belloni T. M., 2011, MNRAS, 410, 679
Ohsuga K., Mineshige S., 2011, ApJ, 736, 2
Dheeraj P. R., Strohmayer T. E., 2012, ApJ, 753, 139
Ponti G., Fender R. P., Begelman M. C., Dunn R. J. H., Neilsen J., Coriat M., 2012, MNRAS, 422, L11
Poutanen J., Lipunova G., Fabrika S., Butkevich A. G., Abolmasov P., 2007, MNRAS, 377, 1187
Rao F., Feng H., Kaaret P., 2010, ApJ, 722, 620
Revnivtsev M., Gilfanov M., Churazov E., Sunyaev R., 2002, A&A, 391, 1013
Roberts T. P., Warwick R. S., Ward M. J., Goad M. R., 2004, MNRAS, 349, 1193
Roberts T. P., 2007, Ap&SS, 311, 203
Shakura N. I., Sunyaev R. A., 1973, A&A, 24, 337
Smith R. K., Brickhouse N. S., Liedahl D. A., Raymond J. C., 2001, ApJ, 556, L91
Stobbart A.-M., Roberts T. P., Wilms J., 2006, MNRAS, 368, 397
Stobbart A.-M., Roberts T. P., Warwick R. S., 2004, MNRAS, 351, 1063
Strohmayer T. E., Mushotzky R. F., 2009, ApJ, 703, 1386
Sutton A. D., Roberts T. P., Middleton M. J., 2013, MNRAS, 435, 1758
Takahashi T., et al., 2010, SPIE, 7732
Takeuchi S., Ohsuga K., Mineshige S., 2013, arXiv, arXiv:1305.1023
Titarchuk L., Shrader C., 2005, ApJ, 623, 362
Walton D. J., Miller J. M., Harrison F. A., Fabian A. C., Roberts T. P., Middleton M. J., Reis R. C., 2013, ApJ, 773, L9
Walton D. J., Miller J. M., Reis R. C., Fabian A. C., 2012, MNRAS, 426, 473
Wilms J., Allen A., McCray R., 2000, ApJ, 542, 914
Winter L. M., Mushotzky R. F., Reynolds C. S., 2007, ApJ, 655, 163
Życki P. T., Done C., Smith D. A., 1999, MNRAS, 309, 561